



Laboratory Investigation of Pullout Behavior of Open-Ended Pipe Helical Soil Nail in Frictional Soil

Pankaj Sharma · Saurabh Rawat · Ashok Kumar Gupta

Received: 27 November 2019 / Accepted: 11 December 2020 / Published online: 2 January 2021
© The Author(s), under exclusive licence to Springer Nature Switzerland AG part of Springer Nature 2021

Abstract In the present work, an experimental study has been conducted to investigate the pullout behavior of helical soil nails fabricated using a hollow pipe with an open end. The main objective of the study is to evaluate the contribution of soil plugging during torque installation and progressive pullout of open-ended helical soil nail (OPHN). The OPHN is installed in a model tank filled with cohesionless soil and subjected to pullout testing. Five different combinations of OPHN varying in shaft diameter (d), helix diameter (D_h), and the number of helices have been used. The test results show that with an increase in D_h/d ratio and surcharge pressure, both installation torque and peak pullout capacity increases. For OPHN, pullout capacity is related to installation torque by a torque coefficient (K_t) varying from 28.12 to 53.3 m^{-1} . The effect of soil plugging is examined in terms of plug length ratio depicting values from 0.19 to 0.28 and constituting 12% of total mobilized shaft friction. The results also depict that installation torque and pullout increase with increasing plug length which depends on ‘ d ’ and is independent of the number of

helices. Smaller soil plug length corresponds to higher axial strains during the pullout of OPHN.

Keywords Open-ended pipe helical nail · Installation · Pullout · Soil plug length · Axial strain

1 Introduction

Soil nailing is a globally accepted technique to strengthen loose soil slopes, fills, and tunnels. Steel rods known as tendons are placed into predrilled cuts or directly driven into the ground surface to a designed depth (Rotte et al. 2013; FHWA 2015; Rawat and Gupta (2016a, b), Rawat 2017, Rawat et al. 2017). This technique achieves recognition because of its great performance under worst-case scenario (Sharma et al. 2019). However, to overcome the shortcomings associated with soil nailing and its installation, helical plates along the nail shaft length are attached to establish an improved form of soil nail termed as helical soil nail (HN). This improved form imparts great pullout strength to HNs due to helical bearing and also facilitated installation without prior drilling or grouting (Rawat and Gupta 2017a; Sharma et al. 2019, 2020). The pullout is considered an important parameter for the internal stability of any soil nail project. To quantify the pullout behavior of HNs, researchers have conducted model tests as well as

P. Sharma · S. Rawat (✉) · A. K. Gupta
Department of Civil Engineering, Jaypee University of
Information Technology, Solan, H.P. 173234, India
e-mail: saurabh.rawat@juit.ac.in

P. Sharma
e-mail: iisc0700ps@gmail.com

A. K. Gupta
e-mail: ashok.gupta@juit.ac.in

numerical modeling on HN with different configurations of shaft diameter, helix diameter, pitch, number of helices, and helical spacing (Sharma et al. 2017; Rawat and Gupta 2017b; Rawat et al. 2017). The results from these studies concluded that a significantly higher pullout is attained for the helical nail in comparison to traditional soil nails with grout.

The review of previous literature also reflects that to increase the installation efficiency during piling, the use of open-ended pipe piles in comparison to closed-end pipe piles in different soil conditions have depicted satisfactory results in terms of bearing and axial load capacity (Paik et al. 2003; Murthy et al. 2018; Seo and Kim 2018; Han et al. 2019). The studies suggested that the phenomenon of soil plugging during driving results in additional internal shaft resistance. Gudavalli et al. 2013 suggested that with pile insertion into the soil, an increase in internal shaft friction is

observed till the complete formation of the soil plug is attained. After soil plugging additional soil is not allowed to enter the pipe and thus increases both the internal resistance and bearing resistance is also mobilized.

Thus, to further improve the installation of HN, the present study incorporates the concept of open-ended pipe piles into the fabrication of open-ended pipe helical soil nails (OPHN). The mechanism of load transfer during pullout of OPHN can be understood from Fig. 1. It can be seen that the pullout force (F) can be equated by three resistance offered from external shaft friction (F_s), internal shaft friction (F_{plug}) due to soil plugging within the hollow pipe, and helical bearing resistance (F_b). The relationship between the resistances can be shown by Eq. (1):

$$F = F_s + F_{plug} + F_b \tag{1}$$

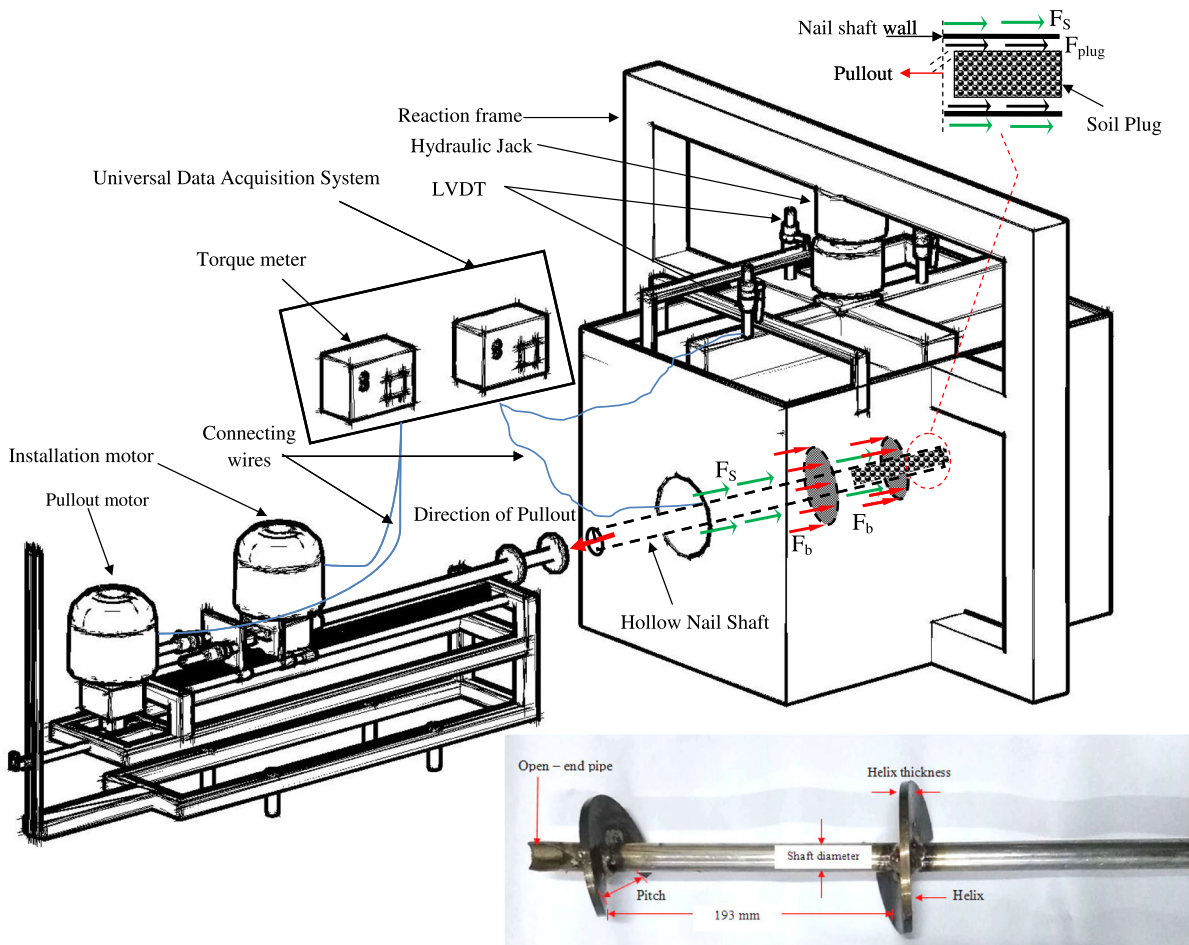


Fig. 1 Detailed testing set-up with load transfer mechanism of open-end helical soil nail (OPHN) and OPHN used in present study

In comparison to traditional soil nails where the pullout resistance is governed by resistance from the tendon-grout interface (F_{sg}) and grout–soil interface (F_{gs}) [Eq. (2)], OPHN depicts higher soil–nail interaction than traditional soil nail.

$$F = F_{sg} + F_{gs} \tag{2}$$

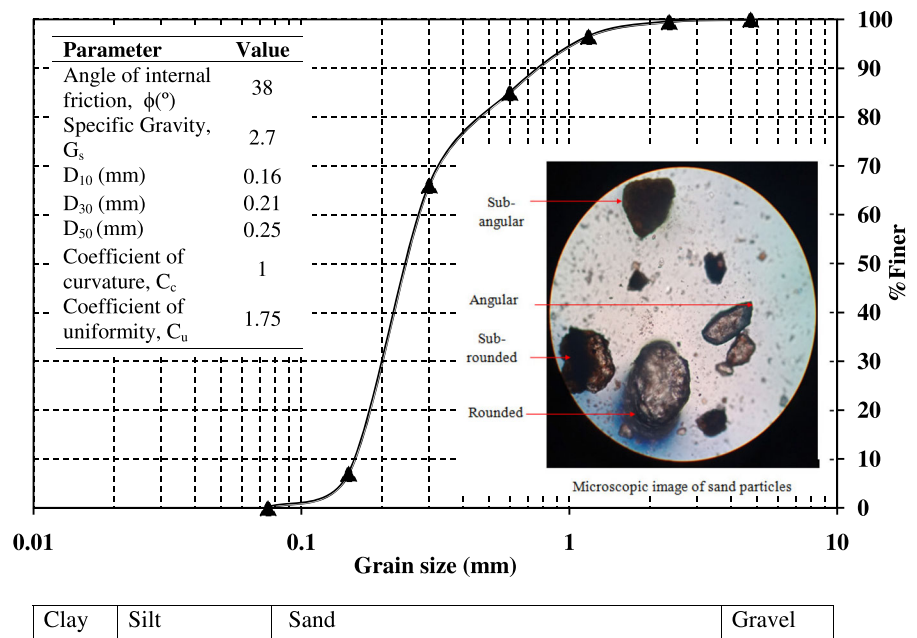
Under this view of enhanced soil–nail interaction using OPHN, the following objectives are determined to evaluate the performance of OPHN used in the present study:

1. To investigate the installation and pullout characteristics of OPHN for five different configurations by varying shaft diameter of a hollow pipe, helix diameter, and the number of helices.
2. Determination of coefficient of torque (K_t) for OPHNs based on test results of torque installation and pullout.
3. To evaluate and quantify the phenomenon of soil plugging during installation and pullout of OPHNs.
4. To study the effect of varying parameters of OPHNs such as hollow shaft diameter, the number of the helix, axial strain, and torsional strain on soil plug length during the pullout.

1.1 Installation and Pullout Testing of OPHNs

The test setup comprises a nail driving device for installation and a displacement control pullout device for pullout testing of OPHNs. A model test tank of dimension 2000 mm × 1100 mm × 1100 mm is used to model the passive soil zone which occurs beyond the slip surface during failure of HNs in actual field condition. The dimensions of the tank are determined such that the minimum tank dimension (i.e. 1100 mm) is greater than ten times the maximum helix diameter (i.e. 90 mm) used. This allows for eliminating the boundary effects during testing. The soil used in the present study reveals rounded, sub-rounded, and angular particles and is classified as poorly graded sand (SP) (Fig. 2) as per IS: 2720 – 4 (1985). Using rainfall technique for attaining a uniform density similar to the field density of $85 \pm 2\%$ filling of the model tank is carried out (Sharma et al. 2020; Vaid and Negussey 1984). To model the in situ stress condition within the model tank, a seating load is applied. For uniform distribution of load, the seating load is applied using an iron plate of 10 mm thickness. For applying the seating as well as surcharge load during later testing, an arrangement consisting of a hydraulic jack and reaction frame is used. The various tests on OPHNs are conducted under varying overburden pressure of 5 kPa, 12.5 kPa, and

Fig. 2 Particle size distribution of soil used. Note D_{50} , average grain size. D_{10} , D_{30} , and D_{60} are the soil grains diameter where 10%, 30% and 60% of the particles are finer than this size respectively



25 kPa depicting stress levels that occur during staged construction in a field of about 2 m. Before OPHN installation, the soil sample was left undisturbed for 24 h to attain a constant stress condition.

The OPHNs used in the present study are modeled with shaft diameter after scaling down shaft diameter used in the field by a factor 5. All OPHNs have a helix thickness and pitch of 8 mm and 24.5 mm, respectively. Schiavon et al. 2016; Sharma et al. 2020 suggest that for no scale effect on test results, the ratio of minimum adopted nail shaft diameter (d) to mean grain size of soil (D_{50}) should be greater than 30. Likewise, the ratio of effective radius of a helix (E) to mean grain size of soil (D_{50}) should be greater than 58. The effective radius of a helix (E) is defined as $0.5(D_h - d)$. Therefore in the present study, the minimum d/D_{50} ratio used is $48 > 30$, and the E/D_{50} ratio used is $72 > 58$. Hence, negligible scale effects on the test results are anticipated. Based on the above-mentioned norms, ‘ d ’ ranging from 12 to 16 mm and ‘ D_h ’ from 48 to 90 mm is adopted. Moreover, to further simplify the installation of OPHNs, increasing the diameter of helical plates was used to form a tapering OPHN (Sharma et al. 2017). The different OPHNs used in the study are presented in Table 1.

The installation of OPHN carried out using a 2 kN-m capacity torque head rotating at a speed of 10 rpm and a crowd force leading to penetration of one pitch per revolution. Once the OPHN are installed to the desired length of 700 mm, the set-up is left for another 24 h. This is done so that stress conditions around OPHN are fully developed before the pullout. Using a displacement controlled pullout apparatus of capacity 50 kN, OPHNs are pullout at a rate of 1 mm/min. The pullout testing is terminated when a percentage

increase of less than 1% is recorded between consecutive pullout values after 1 mm displacement. The instrumentation regarding loading, displacement, and strains is recorded using a Universal Datalogger (UDL). The details and disclaimer of the pullout system are given in Sharma et al. (2020). The complete testing set-up along with model OPHN used in the present study is shown in Fig. 1.

2 Testing Results and Discussions

2.1 Installation Torque and Pullout Force

The installation of hollow helical soil nails is associated with rotation and forward penetration of hollow helical nails. The shearing resistance on nail shaft, helix surface area, and circumference; and bearing resistance from nail end and cutting edge of the helical plate is investigated by observing the variation of installation torque with increasing embedded length up to 700 mm (Fig. 3a). The installation behavior of hollow nails with 1, 2, 3, 4, and 5 helices under an overburden of 25 kPa depicts that higher installation torque is required for nails with a greater number of helical plates. This can be accounted for the increased shearing resistance and bearing resistance found for nails with more helical plates. Similarly, Fig. 3a also reveals that with an increase in the number of the helix, the surrounding soil also undergoes strain-softening (Sharma et al. 2020). This is due to the occurrence of greater soil transversing with more number of helices as the nail penetrates further into the soil. The strain-softening of soil during installation is evident from the zig-zag pattern of ‘4’ and ‘5’ type OPHN shown in Fig. 3a.

The installation torque is also found to vary with increasing shaft diameter. It is evident from Fig. 3a that higher installation torque is attained for 64 mm shaft dia. of ‘3’ type OPHN in comparison to 48 mm shaft dia. For ‘1’ type OPHN. Under varying surcharge pressures of 5 kPa and 12.5 kPa, an identical variation of installation torque is observed. However, between installation torque of OPHN ‘4’ and OPHN ‘3’, approximately a 10% increase is observed. Furthermore, an increase of about 8% is attained with the third helix (OPHN ‘5’) as compared to OPHN ‘4’.

To further investigate the effect of shearing resistance, maximum installation torque is studied against

Table 1 Scheme of experimental program and specifications of open-ended pipe helical nails

Nail sample identification	Shaft diameter (mm)	Internal shaft diameter (mm)	No. of helix	Diameter of helix (mm)
“1”	12	8	1	48
“2”	14	10	1	56
“3”	16	12	1	64
“4”	16	12	2	64 and 90
“5”	16	12	3	64, 90, and 96

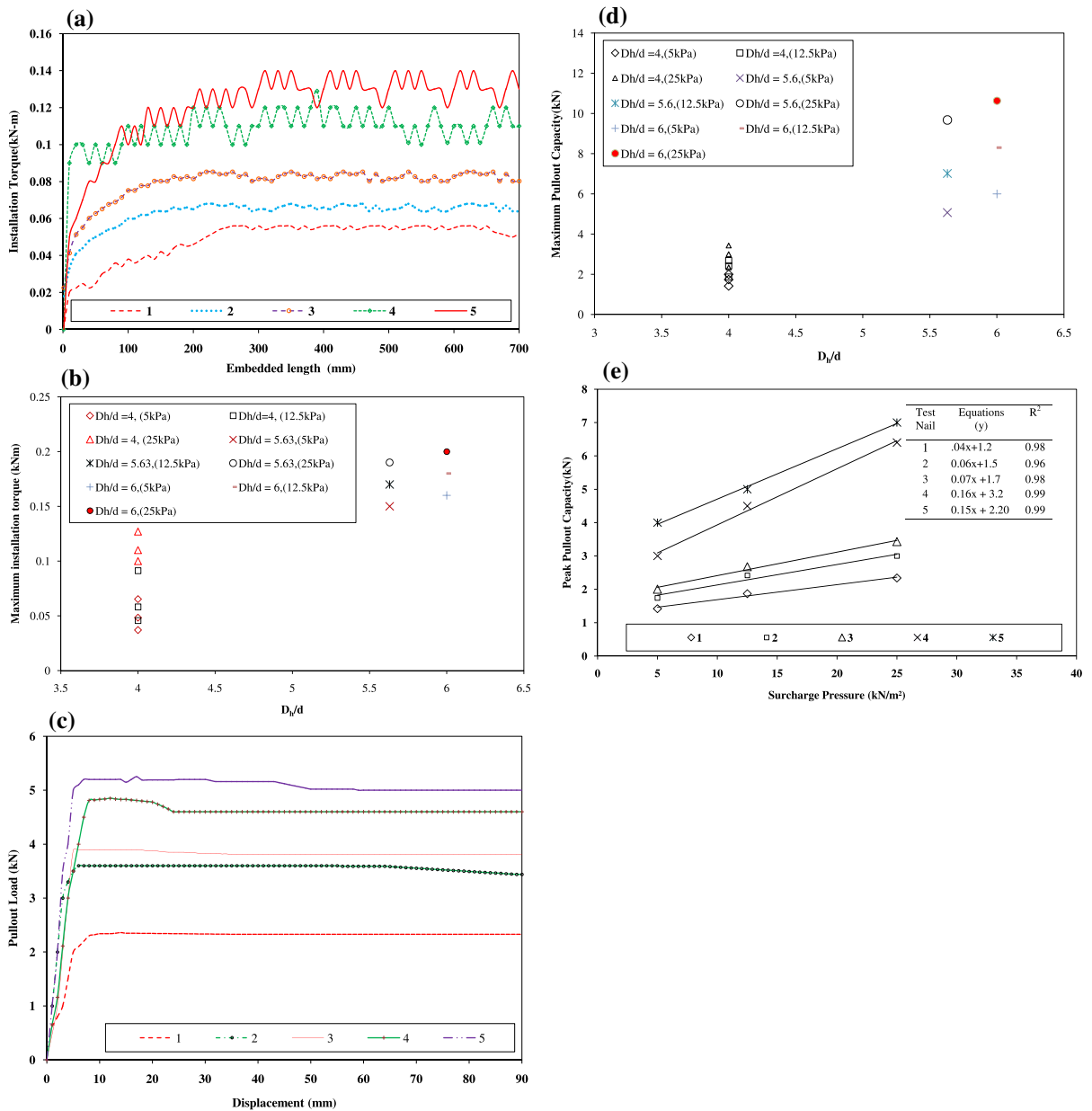


Fig. 3 a Variation of installation torque with embedded length. b Variation of maximum installation torque with D_h/d . c Pullout load–displacement response of different OPHNs under 25 kPa.

d Maximum pullout capacity variation with D_h/d ratio. **e** Variation of peak pullout capacity with surcharge pressure

a non-dimensional parameter (D_h/d) (Hubbell Power Systems Inc. 2018). The non-dimensional parameter (D_h/d) is defined as the ratio of helix diameter to the shaft diameter. It is observed that maximum installation torque increases with an increase in (D_h/d) and surcharge pressure (Fig. 3b). The increase in installation torque is attributed to the enhanced operational

efficiency of the helical element which is related to the D_h/d ratio (Hubbell Power Systems Inc. 2018). It can also be seen that for OPHN with similar efficiency (i.e. same D_h/d ratio), greater maximum installation torque is required for installation under higher surcharge pressure. This is obvious as the OPHN are to be installed against higher confinement which increases

both shearing and bearing resistances offered from the surrounding soil.

As per FSI 2014 torque installation at a rate of fewer than 25 revolutions per minute (rpm) are suggested as ideal for causing minimal soil disturbances. Moreover, it is recommended that for the last 1–1.5 m of installation length of the helical element, a reduction in installation speed less than equal to 10 rpm leads to desirable installation with significantly lesser soil disturbances. Thus, in the present study, all variations of OPHNs are installed at a speed of 10 rpm. To evaluate the soil disturbances caused during installation, ‘Installation disturbance factor (IDF)’ is calculated for all variations of OPHNS based on Eq. (3) modified after Lutenegeger et al. (2014).

$$IDF = \frac{R_{\text{measured}}}{R_{\text{desirable}}} \quad (3)$$

where R_{measured} = Revolution measured per unit advancement of OPHNs; $R_{\text{desirable}}$ = Desirable revolution per unit advancement of OPHNs which is equal to one revolution for one pitch advance. Using Eq. (3), IDF values for different OPHNs are found to vary from 0.70 to 1.53 (Table 2). The IDF values obtained depict minimal disturbances during installation as IDF value 1 or close to 1 reflects installation with an efficiency of 100%. For imperfect helical elements causing significantly large installation disturbances, IDF values s greater than 4 or 5 are reported (Lutenegeger et al. 2014). Therefore, the installation of OPHNs causes negligible disturbances during installation.

Once the OPHN are installed, they were left for 24 h before pullout testing is conducted. This is done to establish the equilibrium in-situ conditions around the installed nails. For OPHN under consideration, pullout capacity is recorded at a point corresponding to an increment in pullout force/1 mm displacement of less than 1% (Zhang et al. 2009). As shown in Fig. 3c,

the pullout behavior of different specimens of OPHN is found to depict a linear increase in the initial portion. As the OPHN is pulled further, the linear behavior fades off into an elastic–plastic behavior. Eventually, on further pullout, complete plastic behavior is observed. The transition of pullout force from elastic to elastic–plastic and finally plastic can be due to the mobilization of shaft resistance as the pullout initiates, which in turn is supported by the helical plate bearing against surrounding soil on further pullout and finally displacement of soil and plate together under constant pullout force leading to permanent soil deformation. Moreover, a higher pullout capacity is obtained for OPHN ‘5’ as compared to OPHN ‘1’ type. Based on this observation it can further be inferred that pullout of OPHN is predominantly governed by the helical bearing instead of shaft friction. Since the shaft surface area in contact with the soil around OPHN will be smaller for OPHN ‘5’ as compared to OPHN ‘1’, the increase in pullout can only be due to the increased bearing offered by an increased number of helical plates. Similarly, the pullout capacity of OPHN increases from the sample “1 to 5” with increasing shaft diameter can also be attributed to the increased surface area and consequently increased circumferential shaft friction around by large diameter.

In addition, peak pullout capacity is also found to vary with the D_h/d ratio defined as wing ratio for examining the contribution of helix diameter to shaft diameter during OPHN pullout. As seen from Fig. 3d, pullout capacity is found to be increase with an increase in the D_h/d ratio. Thus, it can be deduced that with an increase in shaft diameter and helix diameter, both bearing and shearing resistance increases. Moreover, as surcharge pressure increases from 5 to 12.5 kPa and finally to 25 kPa, confining pressure increases the resistance (shearing and bearing) from

Table 2 Maximum plug length and maximum pullout capacity (under 25 kPa)

Test nail	Maximum plug length (m)	Maximum pullout capacity (kN)	IDF	Recommendation (Lutenegeger et al. 2014)
“1”	0.087	2.34	1.28–1.53	No disturbance IDF = 1
“2”	0.104	3	1.23–1.37	Large disturbance IDF > 4
“3”	0.108	3.43	1.09–1.33	
“4”	0.109	6.4	0.98–1.25	
“5”	0.11	7	0.70–0.90	

the surrounding soil, thus depicting better pullout capacity.

Moreover, as per Perko (2009), for design pullout capacity of helical components, a reduction factor ‘ λ ’ equal to 0.87 is used to account for the soil disturbances based on field data. However, the ‘ λ ’ value is greatly governed by the in-situ soil conditions and efficiency of installation done. The present study reveals significantly high installation efficiency ranging from 0.70 to 1.53, and thus a reduction factor ‘ λ ’ > 0.87 can be assumed. This means that soil disturbances have an insignificantly small effect on nail pullout capacity.

The variation of pullout capacity of different OPHN under increasing surcharge pressures of 5 kPa, 12.5 kPa, and 25 kPa is shown in Fig. 3e. It can be observed that the pullout capacity can be treated in terms of shear stress by dividing it with the area of OPHN and surcharge pressures can be treated as variation in normal stresses. Thus, it can be seen that a linear variation of pullout capacity under increasing surcharge pressure is obtained which is identical to Mohr–Coulomb failure criterion. A similar correlation has also been reported by Tokhi et al. (2017), Sharma et al. (2017) and Sharma et al. (2020) for screw and solid shaft helical nails, respectively.

2.2 Torque Coefficient (K_t) for OPHNs

The relationship between pullout capacity and installation torque is adopted based on the empirical relationship suggested by Hoyt and Clemence (1989) and given by Eq. (4) as:

$$Q_u = K_t \cdot T \quad (4)$$

In Eq. (4), the highest pullout capacity of the helical element is denoted by Q_u and maximum installation torque is denoted by T . Based on the field observations, Eq. (4) suggested that the pullout capacity of a helical nail corresponds to the maximum installation torque applied during installation and is related by a parameter known as Torque coefficient (K_t). However, as observed from previous literature, K_t values can only be found for closed and open-ended helical piles and helical anchors (Ghaly et al. 1991; Perko 2009; Sakr 2015). Very few literature exists which have reported or investigated K_t for helical soil nails (Sharma et al. 2018a, b, c, 2020). However, as per the best of the authors’ knowledge, the investigation of

K_t for OPHN is non-existent. The investigation of K_t for OPHN is significant as it also incorporates the effect of soil plugging encountered during installation. It is found that OPHN pullout and installation torque increase with an increase in surcharge pressure. Moreover, pullout capacity and installation torque also vary with different configurations of OPHN. Thus, the average K_t value has been presented which is found to vary from 28.12 to 53.3 m^{-1} for OPHN ‘1’ to OPHN ‘5’. Even though K_t is a coefficient, it is not a constant because it is weakly governed by the number of helical plates, helical plate radius and largely dependent on soil properties, shaft diameter, and helix thickness. Moreover, the reliability of pullout capacity and installation torque method is reported as 97.7% (Hubbell Power Systems 2018), hence further authenticating the K_t values attained for the present work.

2.3 Soil Plugging in OPHNs

The soil plugging performance was documented by Kishida and Isemoto (1977) in the context of piles modeled using pipes with open ends. The soil plugging behavior is investigated in terms of plug length ratio (PLR) and incremental filling ratio (IFR) as suggested by Paik et al. (2003) and Gudavalli et al. (2013) and is defined by Eqs. (5) and (6):

$$\text{Plug Length Ratio} = \frac{S_L}{N_L} \quad (5)$$

$$\text{Incremental Filling Ratio} = \frac{\Delta S_L}{\Delta N_L} \quad (6)$$

where N_L = nail penetration level; S_L = soil plug; ΔN_L = increase in penetration of nail; and ΔS_L = increase in soil plugging with increasing nail penetration (see Fig. 4a). As evident from Fig. 4a, when nail penetration length becomes equal to soil plug length then plug length ratio and the incremental filling ratio becomes equal to 1. In addition, when soil plug length becomes constant, then IFR equal to 0, whereas the plug length ratio is not necessarily 0 at the same level. During laboratory testing, the formation of the length of soil plug in all samples of OPHN was recorded after every 50 mm penetration during installation (Table 3). A calibrated steel rod of diameter 3 mm is inserted from the nail head into the hollow shaft nail after every 50 mm penetration during installation. From Table 3, it is clear that as nail penetration

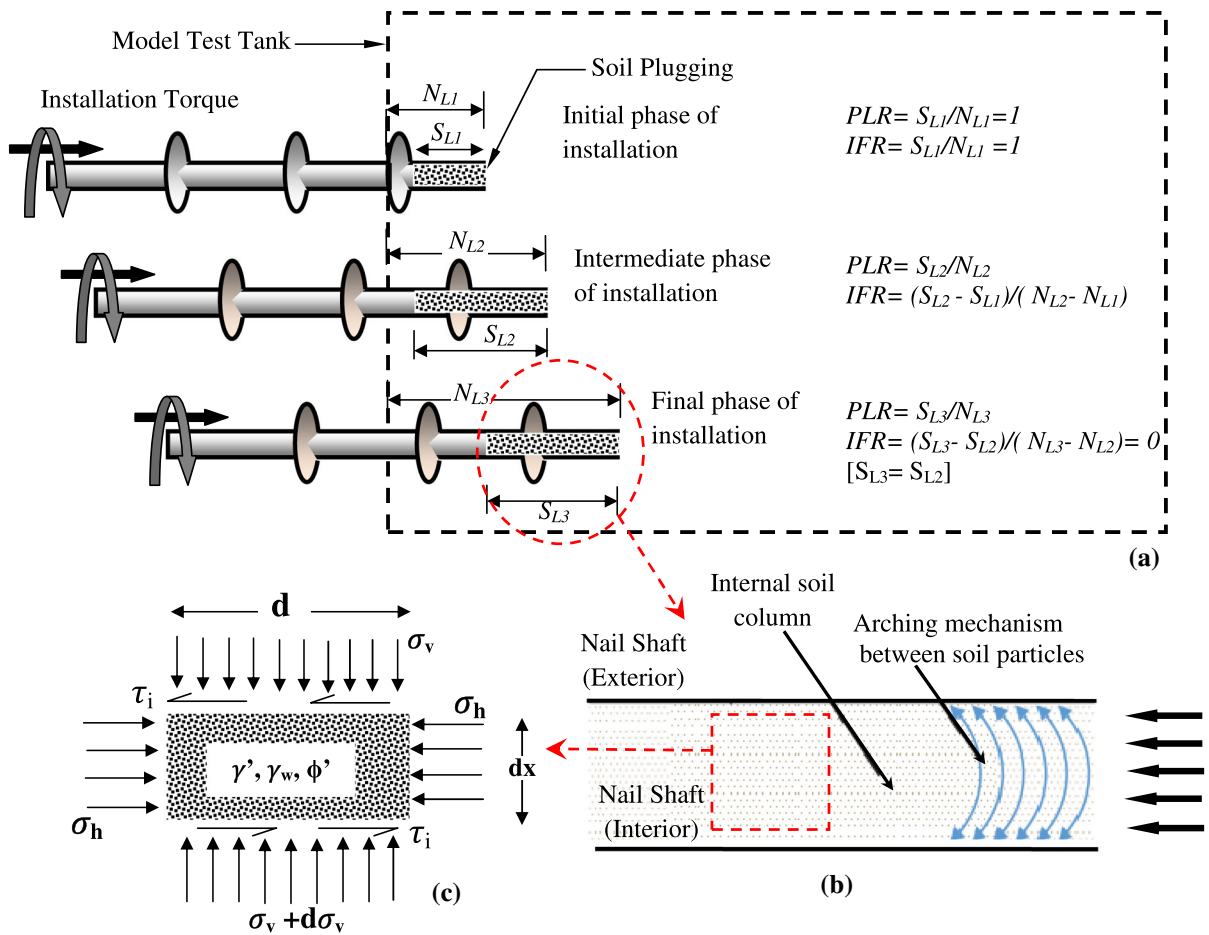


Fig. 4 Soil plugging **a** with installation progress **b** sketch of arching principle **c** stresses acting on wedge

reaches 0.45–0.50 m of nail length, 80–100 mm length of soil plugging occurs which then becomes constant (at 25 kPa). It is observed that soil plugging contributes to the total frictional resistance mobilized during installation which consequently contributes 12% to the total shaft friction (external + internal) acting during the pullout. It is observed that as the soil plug length of OPHN increases, the pullout capacity of the nail also increases (Table 2). For nail samples ‘3’ to ‘5’, less than 1% increment in soil plug length is recorded which is almost negligible. Based on this observation, it can be concluded that an increase in the number of helices does not influence the soil plug length. Moreover, from Table 3, it can also be deduced that soil plug length primarily depends upon the shaft diameter and is independent of the number of the helix. Table 3 also shows that OPHN with a large

diameter incorporates greater soil plug length because of the ease of soil movement into the hollow shaft during nail penetration.

The IFR values are found to be varying continuously and after 0.45–0.50 m of nail penetration, the IFR value becomes equal to zero (Table 3). This can be accounted to the fact that after 0.45–0.50 m of OPHN penetration, soil plug length becomes constant and restrains any further movement of soil into the hollow shaft. Thus, it can be accomplished that the incremental filling ratio entirely depends on the soil plug length.

The mechanism for redistribution of stresses within the soil body during plugging is attributed to arching in cohesionless soils (Paikowsky 1989). The arching mechanism also governs the pullout behavior of soil in a laterally confined space. During the installation of OPHN, soil arching causes concave soil formation at

Table 3 Summary of experimental result of PLR and IFR (under 25 kPa)

Specimens	Length of soil plug (m)	Nail penetration depth (m)	PLR	IFR	
	0	0			
“1”	0.015	0.05	0.30	0.4	
	0.035	0.1	0.35	0.3	
	0.05	0.15	0.33	0.44	
	0.072	0.2	0.36	0.16	
	0.08	0.25	0.32	0.04	
	0.082	0.3	0.27	0.04	
	0.084	0.35	0.24	0.02	
	0.085	0.4	0.21	0.04	
	*	0.087	0.45	0.19	0
		0.087	0.5	0.17	0
0.087		0.55	0.16	0	
0.087		0.6	0.15	0	
0.087		0.65	0.13	0	
0.087		0.7	0.12		
“2”	0	0			
	0.02	0.05	0.40	0.46	
	0.043	0.1	0.43	0.42	
	0.064	0.15	0.43	0.36	
	0.082	0.2	0.41	0.22	
	0.093	0.25	0.37	0.1	
	0.098	0.3	0.33	0.04	
	0.1	0.35	0.29	0.02	
	0.101	0.4	0.25	0.06	
	*	0.104	0.45	0.23	0
0.104		0.5	0.21	0	
0.104		0.55	0.19	0	
0.104		0.6	0.17	0	
0.104		0.65	0.16	0	
0.104		0.7	0.15		
“3”	0	0			
	0.025	0.05	0.50	0.4	
	0.045	0.1	0.45	0.5	
	0.07	0.15	0.47	0.3	
	0.085	0.2	0.43	0.22	
	0.096	0.25	0.38	0.16	
	0.104	0.3	0.35	0.04	
	0.106	0.35	0.30	0.04	
	*	0.108	0.4	0.27	0
		0.108	0.45	0.24	0
0.108		0.5	0.22	0	
0.108		0.55	0.20	0	
0.108		0.6	0.18	0	

Table 3 continued

Specimens	Length of soil plug (m)	Nail penetration depth (m)	PLR	IFR	
	0.108	0.65	0.17	0	
	0.108	0.7	0.15		
“4”	0	0			
	0.027	0.05	0.54	0.42	
	0.048	0.1	0.48	0.5	
	0.073	0.15	0.49	0.28	
	0.087	0.2	0.44	0.26	
	0.1	0.25	0.40	0.1	
	0.105	0.3	0.35	0.02	
	0.106	0.35	0.30	0.06	
	*	0.109	0.4	0.27	0
		0.109	0.45	0.24	0
0.109		0.5	0.22	0	
0.109		0.55	0.20	0	
0.109		0.6	0.18	0	
0.109		0.65	0.17	0	
	0.109	0.7	0.16		
“5”	0	0			
	0.027	0.05	0.54	0.0042	
	0.048	0.1	0.48	0.005	
	0.073	0.15	0.49	0.0028	
	0.087	0.2	0.44	0.0026	
	0.1	0.25	0.40	0.001	
	0.105	0.3	0.35	0.0004	
	0.107	0.35	0.31	0.0006	
	*	0.11	0.4	0.28	0
		0.11	0.45	0.24	0
0.11		0.5	0.22	0	
0.11		0.55	0.20	0	
0.11		0.6	0.18	0	
0.11		0.65	0.17	0	
	0.11	0.7	0.16		

*Nail penetration level beyond which, IFR = 0

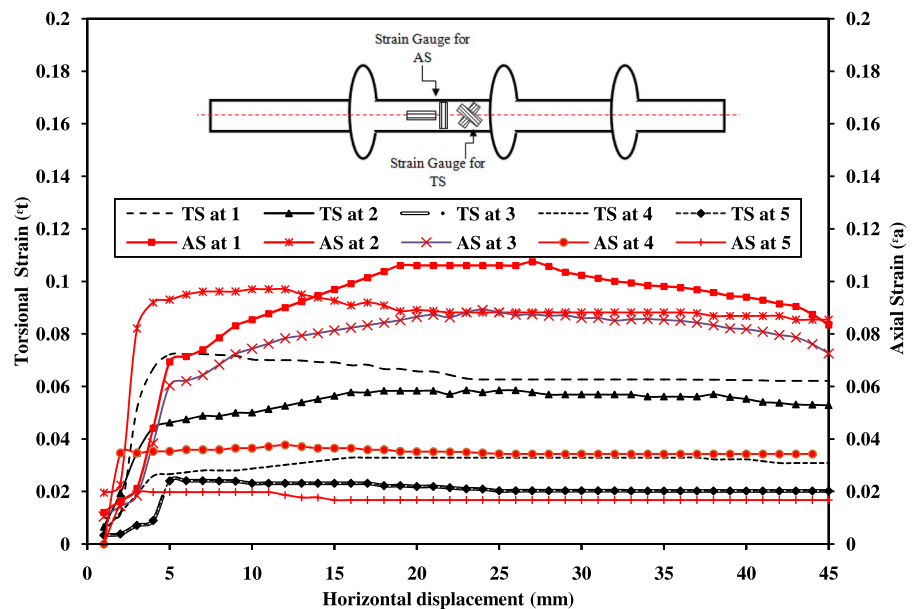
the nail toe level (Fig. 4b). Due to this, axial stress acting on the internal soil column at the toe of the nail is transmitted to the nail walls in the form of normal stress and shear stresses, resulting in increased internal shaft friction (Fig. 4c). Thus, as depicted in Eq. (1), resistance due to soil plug (F_{plug}) is mobilized as pullout progresses in addition to outer shaft friction (F_s) and bearing resistance from helical plates (F_b).

2.4 Effect of Soil Plugging on Torsional Strain (TS) and Axial Strain (AS) During the Pullout

During pullout of a hollow helical nail, torsional strains and axial strains are investigated using two pairs of strain gauges each fixed at the center of the nail shaft length. As per Omega (2019), torsional strains along the nail shaft is measured by placing two strain gauges perpendicular to each other on either side of the shaft. Similarly, with one strain gauge along the longitudinal axis of the shaft and the other perpendicular to it, axial strains developed during pullout are recorded (Fig. 5). It is obvious and evident from Fig. 5 that as the nail is pulled out, axial strains are developed. However, the developed axial strains are found to be significantly higher for hollow helical nails with a diameter range of 12 mm–16 mm having a single helix as compared to 16 mm diameter shaft with 2 or 3 helices. This behavior of developed axial strains can be attributed to the relatively small resistance mobilized by the nails with 1 helix as compared to 2 or 3 helices. On comparing, it can be understood that on pulling along with shaft frictions, hollow nails also resist by bearing imposed from helical plates. Since bearing from 1 helix is smaller as compared to 2 and 3 helices, the nail pulls out relatively easily as compared to its counterparts, thereby depicting larger axial strains. Moreover, another rationale can be the plugging effect developed during nail installation. It can be examined that 12 mm

diameter hollow nail with 1 helix depicts a smaller plug length of 87 mm in comparison to 16 mm diameter hollow nail with 3 helices having plug length of 110 mm. Thus, it can be stated that large axial strains are developed in hollow nails with smaller plug length. One striking feature that can be observed from Fig. 5 is the development of torsional strains. This brings out the fact that during pullout, helical nails are found to undergo rotation as well. The reason for the observed rotation can be contributed to the path traced by the helix during installation. Since a smaller diameter of the helical path is easily retractable as compared to a larger path, higher torsional strains can be found for hollow nails with 48 mm helix than 64 mm helix. Moreover, for tapered multi-helix such as 64 and 90 mm, path retracing is relatively difficult, hence developed torsional strains are significantly small. However, a contradiction is observed for torsional strain developed in 16 mm hollow nail with 1 helix which is smaller than 16 mm multi-helix with 64 and 90 mm helices. The reason can be the observed horizontal displacement of 45 mm during with only the contribution of 64 mm helix is reflected. Similar to axial strains, torsional strains are also found to be larger for small soil plug lengths as compared to larger plug lengths. Hence it can be summarized that for hollow helical nails larger axial and torsional strains are developed for nails with small soil plug length, smaller shaft diameter, and less number of helical plates.

Fig. 5 Variation of torsional strain and axial strain with horizontal displacement during pullout under overburden of 25 kPa



3 Conclusions

In the present study, a series of model tests using five different configurations of OPHNs are conducted to evaluate the installation and pullout behavior under varying surcharge pressure between 5 kPa to 25 kPa. The effect of soil plugging on OPHN installation and pullout is also recorded during testing. The soil plugging phenomenon is quantified in terms of PLR and IFR. The axial and torsional strains developed during pullout are also related to the length of the soil plug. Based on the test results obtained, it can be concluded that installation and pullout of OPHN increases with open-ended pipe diameter, D_h/d ratio, and surcharge pressure. The torque coefficient (K_t) values obtained for OPHNs vary from 28.12 to 53.3 m^{-1} depicting installation torque to pullout capacity relationship under-reported literature. The effect of soil plug is also found to govern the installation and pullout of OPHNs. Soil plugging is found to occur up to shaft penetration of 0.45 m–0.5 m beyond which the IFR value becomes zero. Soil plug length is directly proportional to the open-ended pipe diameter and is independent of the number of helices. It is also found that larger soil plug length corresponds to higher installation torque and pullout capacity of OPHNs. From the analysis of results, it is concluded that soil plug length contributes to 12% of the total pullout resistance with the remaining 88% resistance being achieved from the external shaft friction and bearing from helical plates. The variation of axial strains depicts that smaller diameter OPHNs with less number of helices corresponds to smaller soil plug length and consequently large axial strains during the pullout. From the recorded torsional strains during pullout, it can be concluded that OPHNs undergo partial rotation along with horizontal displacement. The torsional strains depict an identical relationship with soil plug length, OPHN diameter, and helix number as axial strains.

Funding Not applicable.

Availability of data and materials All data and material has been included in the text. Code availability Not applicable.

Compliance with ethical standards

Conflict of interest On behalf of the co-authors, the corresponding authors declares no conflict of interest.

References

- FHWA (2015) Geotechnical engineering circular No. 7: Soil nail walls—reference manual. FHWA, Washington, D.C. Rep. No. FHWA-NHI-14-007
- FSI (2014) Technical manual: helical piles and anchors, hydraulically driven push piers, polyurethane injection & supplemental support systems, 2nd edn. Foundation Support Works, Omaha, pp 33–39
- Ghaly A, Hanna A, Hanna M (1991) Installation torque of screw anchors in sand. *Soils Found* 31(2):77–92. https://doi.org/10.3208/sandf1972.31.2_77
- Gudavalli SR, Safaqaq O, Seo H (2013) Effect of soil plugging on axial capacity of open-ended pipe piles in sands. In: Proceedings of 18th international conference on soil mechanics and geotechnical engineering, Paris, pp 1487–1490. <http://www.cfms-sols.org/sites/default/files/Actes/1487-1490.pdf>
- Han F, Ganju E, Salgado R, Zaheer M (2019) Axial resistance of open-ended pipe pile driven in gravelly sand. *Geotechnique*. <https://doi.org/10.1680/jgeot.18.P.117>
- Hoyt RM, Clemence SP (1989) Uplift capacity of helical anchors in soil. In: Proceedings 12th international conference on soil mechanics and foundation engineering, Brasil, vol 2, pp 1019–1022
- Hubbell Power Systems, Inc. (2018) HUBBELL Technical Design Manual Edition 4. Chance Atlas
- IS: 2720 – 4 (1985) Grain size analysis. Bureau of Indian Standard (BIS), New Delhi
- Kishida H, Isemoto N (1977) Behaviour of sand plugs in open-end steel pipe piles. In: Proceedings of the 9th international conference on soil mechanics and foundation engineering, Tokyo, pp 605–608
- Lutenegger AJ, Erickson J, Williams N (2014) Evaluating installation disturbance of helical anchors in clay from field vane tests. In: Proceedings of DFI annual meeting 2014
- Murthy DS, Robinson RG, Rajagopal K (2018) Formation of soil plug in open-ended pipe piles in sandy soils. *Int J Geotech Eng*. <https://doi.org/10.1080/19386362.2018.1465742>
- Omega.co.uk (Strain gages manual) (2019) Positioning strain gages to monitor bending, axial, shear, and torsional loads: a guide to installation (E56). <http://www.personal.umich.edu/bkerkez/courses/cee575/Handouts/2strainpositioning.pdf>. Accessed 2019
- Paik K, Salgado R, Lee J (2003) Determination of bearing capacity open ended piles in sand. *J Geotech Geoenviron Eng* 129(1):46–57
- Paikowsky S (1989) A static evaluation of soil plug behavior with application to the pile plugging problem. MIT, Cambridge
- Perko HA (2009) Helical piles: a practical guide to design and installation. Wiley, Hoboken

- Rawat S (2017) Testing and modeling of soil-nailed slopes. PhD Thesis, Jaypee University of Information Technology, Wanknaghat, Solan, Himachal Pradesh, India
- Rawat S, Gupta AK (2016a) An experimental and analytical study of slope stability by soil nailing. *Electron J Geotech Eng* 21(17):5577–5597
- Rawat S, Gupta AK (2016b) Analysis of nailed soil slope using limit equilibrium and finite element methods. *Int J Geosynth Ground Eng* 2(4):34. <https://doi.org/10.1007/s40891-016-0076-0>
- Rawat S, Gupta AK (2017a) Testing and modeling of screw nailed soil slopes. *Indian Geotech J* 48(1):52–71
- Rawat S, Gupta AK (2017b) Numerical modelling of pullout of helical soil nail. *J Rock Mech Geotech Eng* 9(4):648–658. <https://doi.org/10.1016/j.jrmge.2017.01.007>
- Rawat S, Gupta AK, Kumar A (2017) Pullout of soil nail with circular discs: a three-dimensional finite element analysis. *J Rock Mech Geotech Eng* 9:967–980
- Rotte V, Viswanadham B, Chourasia D (2013) Influence of slope geometry and nail parameters on the stability of soil-nailed slopes. *Int J Geotech Eng*. <https://doi.org/10.3328/IJGE.2011.05.03.267-281>
- Sakr M (2015) Relationship between installation torque and axial capacities of helical piles in cohesionless soils. *Can Geotech J* 52(6):747–759
- Schiavon J, Tsuha C, Thorel L (2016) Scale effect in centrifuge tests of helical anchors in sand. *Int J Phys Model Geotech* 16(4):185–196. <https://doi.org/10.1680/jphmg.15.00047>
- Seo H, Kim M (2018) Soil plug behaviour of open-ended pipe piles during installation. *J Deep Found Inst*. <https://doi.org/10.1080/19375247.2018.1448552>
- Sharma M, Samanta M, Sarkar S (2017) A laboratory study on pullout capacity of helical soil nail in cohesionless soil. *Can Geotech J* 54(10):1482–1495
- Sharma M, Samanta M, Sarkar S (2018a) Novel laboratory pullout device for conventional and helical soil nails. *Geotech Test J (ASTM)* 42(5):1–23. <https://doi.org/10.1520/GTJ20170319>
- Sharma P, Rawat S, Gupta AK (2018b) Study and remedy of Kotropi Landslide in Himachal Pradesh, India. *Indian Geotech J* 48(4):1–17. <https://doi.org/10.1007/s40098-018-0343-1>
- Sharma P, Rawat S, Gupta AK (2018c) Remedy measure for the Kotropi Landslide (Mandi, H.P.) India: a case study. *J Civ Eng Environ Technol* 5(3):125–128
- Sharma M, Samanta M, Punetha P (2019) Experimental investigation and modeling of pullout response of soil nails in cohesionless medium. *Int J Geomech ASCE* 19(3):04019002-1–04019002-16
- Sharma P, Rawat S, Gupta AK (2020) Horizontal pullout behavior of novel open-ended pipe helical soil nail in frictional soil. *Int J Civ Eng*. <https://doi.org/10.1007/s40999-020-00535-2>
- Tokhi H, Ren G, Li J (2017) Laboratory pullout resistance of a new screw soil nail in residual soil. *Can Geotech J* 55(5):609–619. <https://doi.org/10.1139/cgj-2017-0048>
- Vaid YP, Negussey D (1984) Relative density of pluviated sand samples. *Soils Found Jpn Soc Soil Mech Found Eng* 24(2):101–105. https://doi.org/10.3208/sandf1972.24.2_101
- Zhang LL, Zhang LM, Tang WH (2009) Uncertainty of field pullout resistance of soil nails. *J Geotech Geo-environ Eng* 135(7):966–972. [https://doi.org/10.1061/\(ASCE\)GT.1943-5606.0000014](https://doi.org/10.1061/(ASCE)GT.1943-5606.0000014)

Publisher's Note Springer Nature remains neutral with regard to jurisdictional claims in published maps and institutional affiliations.